

# Solving the PIHNA model while accounting for radiotherapy

Alexandros Roniotis, Vangelis Sakkalis, Eleftheria Tzamali, Georgios Tzedakis, Michalis Zervakis, and Kostas Marias

**Abstract**— Glioblastoma is the most aggressive type of glioma. During the last decades, several models have been proposed for simulating the growth procedure of glioma. One of the latest proposed models builds upon the proliferation – diffusion model by incorporating the angiogenic net rates and different concentration of cell populations (normoxic, hypoxic and necrotic). This proliferation- invasion- hypoxia- necrosis- angiogenesis model (PIHNA) does not take into account radiotherapy. This work presents the mathematical foundation for solving PIHNA model in two dimensions with incorporated radiotherapy effect using the Linear Quadratic Model, which uses radiobiology parameters.

## I. INTRODUCTION

GLIOMA, especially glioblastoma, is the most fatal brain cancer, despite the major advances in medicine [1-3]. The highly invasive and neoplastic growth of glioma has emerged the necessity to describe the mechanism of glioma growth, using mathematical models.

The major macroscopic models either use the diffusion reaction equation for simulating the change of tumor cell concentration (diffusive models) [4-9] or cellular automata for simulating invasion and proliferation by using deterministic cell state change rules [10-11].

This paper deals with an extended type of diffusive models for three types of cell populations and simulates radiotherapy by adding a consuming term from the Linear Quadratic Model in the respective equations.

## II. BACKGROUND

Diffusive models [4] simulate the change of glioma concentration in time and in space, by using two main terms for invasion (diffusion term) and proliferation (reaction term) of glioma cells. The equation used in diffusive models is the following:

$$\frac{\partial c}{\partial t} = \nabla \cdot (D \nabla c) + \rho c \left(1 - \frac{c}{k}\right) \quad (1)$$

where  $c(\mathbf{x}, t)$  is the tumor concentration in position  $\mathbf{x}$  at time  $t$ ,  $D$  is the diffusion coefficient (can be spatially varying),  $\nabla$  and  $\nabla \cdot$  are the gradient and divergence operators

Manuscript received September 1, 2012. This work was supported in part by the community initiative Program INTERREG III, Project “YIIEPΘEN”, financed by the European Commission through the European Regional Development Fund and by National Funds of Greece and Cyprus and the EC project TUMOR (FP7-ICT-2009.5.4-247754)

A. Roniotis, V. Sakkalis, E. Tzamali, G. Tzedakis and K. Marias are with the Institute of Computer Science, FORTH, Vassilika Vouton, GR-70013 Heraklion, Crete, Greece ({roniotis; sakkalis; tzamali; gtzedaki; kmarias}@ics.forth.gr).

A. Roniotis and M. Zervakis are with the Dept of Electronic & Computer Engineering, Technical University of Crete, 73100, Chania, Greece (michalis@display.tuc.gr).

respectively,  $\rho$  is the net cell proliferation rate and  $k$  is the maximum tumor cell concentration. This model assumes that cancerous cells proliferate at a constant rate which is independent of nutrients availability and the cell population has the same type.

In order to incorporate nutrient availability and oxygenation, the model of (1) can be altered to the proliferation- invasion- hypoxia- necrosis- angiogenesis (PIHNA) model [12-13]. This model includes three different types of cell population, normoxic, hypoxic and necrotic, while vasculature and angiogenic factors (e.g. VEGF) have also been incorporated into the model.

The emerging system of equations for these three types of cells, endothelial cells (vasculature) and angiogenic factors are:

$$\begin{aligned} \frac{\partial c}{\partial t} &= \nabla \cdot (D(1-T)\nabla c) + \rho c(1-T) + \gamma hV - \beta c(1-V) - a_n n c \\ \frac{\partial h}{\partial t} &= \nabla \cdot (D(1-T)\nabla h) - \gamma hV + \beta c(1-V) - (a_h(1-V) + a_n n)h \\ \frac{\partial n}{\partial t} &= a_n h(1-V) + a_n n(c+h+v) \end{aligned} \quad (2)$$

$$\frac{\partial v}{\partial t} = \nabla \cdot (D_v(1-T)\nabla v) + \mu \frac{a}{K_m + a} v(1-T) - a_n n v$$

$$\frac{\partial a}{\partial t} = \nabla \cdot (D_a \nabla a) + \delta_c c + \delta_h h - q \mu \frac{\alpha}{K_m + \alpha} v(1-T) - \omega a v - \lambda a$$

where  $V = v/(c+h+v)$ ,  $T = (c+h+v+n)/k$ . In first equation  $c(\mathbf{x}, t)$  is the concentration of normoxic cells at position  $\mathbf{x}$  at time  $t$ . The cells diffuse at a rate  $D$ , proliferate at a rate  $\rho$ , turn to hypoxic at a rate  $\beta$  or turn directly to necrotic (due to contact death) at a rate  $a_n$ .

Similarly,  $h(\mathbf{x}, t)$  is the concentration of hypoxic cells, which diffuse at a rate  $D$ , turn back to normoxic at a rate  $\gamma$  or turn to necrotic at a rate  $a_h$ .

Continuing,  $n(\mathbf{x}, t)$  is the concentration of necrotic cells, while  $v(\mathbf{x}, t)$  and  $a(\mathbf{x}, t)$  are the vasculature (endothelial cells linked to oxygenation) and concentration of angiogenic factors, respectively. Vasculature disperses at a rate  $D_v$ , increases at a rate  $a_v = \mu \frac{a}{K_m + a}$  and turns to necrotic cells at rate  $a_n$ .

Lastly, angiogenic factors are produced by normoxic cells at rate  $\delta_c$  and by hypoxic cells at rate  $\delta_h$ , decay at a rate  $\lambda$  and are washed out by vessels at rate  $\omega$ . In the last two equations,  $\mu$  is the proliferation rate of endothelial cells,  $K_m$  is the Michaelis – Menten constant of response of endothelial cells to angiogenic factors and  $q$  is the consumption of angiogenic factors per endothelial cell proliferation.

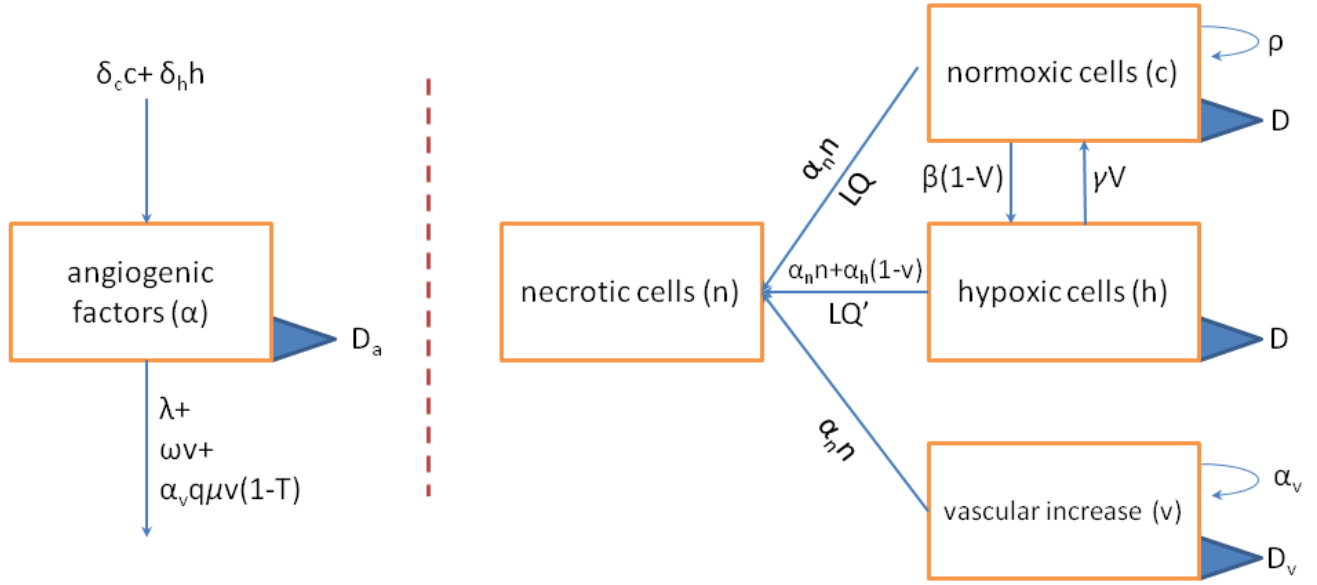


**Fig. 1. Modified Figure from [13]: Outline of the PIHNA-LQ mathematical interactions for the PIHNA model, by adding the radiotherapy terms extracted from the LQ model [16]. The interactions interfere normoxic cells, hypoxic cells, necrotic cells, endothelial cells (vasculature) and angiogenic factors (e.g. VEGF).**

In order to incorporate radiotherapy into the PIHNA model, the Linear Quadratic Model (LQ) could be used [14-17]. According to LQ model, the probability of cells surviving  $S$  following a single dose of radiation  $R(\mathbf{x}, t)$  was observed to follow the relationship:

$$S(R) = \exp(-AR - BR^2) \quad (3)$$

where *linear*  $A$  and *quadratic*  $B$  are the radiobiology parameters, which are interpreted biologically as repairable single and lethal double-strand breaks to the cell's DNA, respectively [15]. In general, cancers with high motility, like glioblastoma, show a high tissue response  $A/B \approx 10$  [16]. Especially for photon radiation therapy, which is most commonly applied, the hypoxic cells are as much as 2 to 3 times more resistant to radiation damage than normoxic [18]. Thus, Oxygen Enhancement Ratio ( $OER$ ) has to be included in the model [19].

### III. METHODS

This paper investigates the incorporation of radiotherapy effect in the PIHNA model. Radiotherapy could be interpreted as an additional term for turning normoxic cells and hypoxic cells to necrotic cells in the first two equations of (2). Given the radiotherapy dose, the effectiveness of irradiation on hypoxic cells, compared to normoxic cells, is lower and this is expressed through  $OER$ . Thus, if we assume that all normoxic cells are affected by irradiation and  $OER$  is the Oxygen Enhancement Ratio, then the first three equations of (2) can be altered to the PIHNA-LQ model as following:

$$\frac{\partial c}{\partial t} = \nabla \cdot (D(1-T)\nabla c) + \rho c(1-T) + \gamma h V - \beta c(1-V) - a_n n c - LQc$$

$$\frac{\partial h}{\partial t} = \nabla \cdot (D(1-T)\nabla h) - \gamma h V + \beta c(1-V) - (a_h(1-V) + a_n n)h - LQ'h$$

$$\frac{\partial n}{\partial t} = a_h h(1-V) + a_n n(c+h+v) + LQ'h + LQc \quad (4)$$

where:

$$LQ = 1 - e^{-AR(t) - BR^2(t)} \quad (5)$$

$$LQ' = 1 - e^{-\frac{A}{OER}R(t) - \frac{B}{OER^2}R^2(t)}$$

Fig.1. illustrates the interactions between the elements of the PIHNA-LQ model for simulating proliferation, invasion, hypoxia, necrosis, angiogenesis and radiotherapy. The interactions have been extracted from equations (2), (4), (5). The diagram has been designed on the diagram of Figure 1 of [13], by adding the radiotherapy terms of the LQ model.

### IV. MODEL IMPLEMENTATION

We have implemented the PIHNA-LQ model in MathWorks™ Matlab (version 7.1). As there is no direct algebraic solution to the equation system of (4), we estimated the solution numerically. More specifically, we approximated the spatiotemporal solution of the system of the five partial differential equations by developing numerical schemes of Finite Differences in two spatial dimensions.

In order to avoid instability issues, the implicit numerical method of Crank Nikolson was used for building the Finite Differences for a variable in an equation where this variable was subject to temporal change.

On the other hand, in order to simplify the procedure of solving, an explicit method (Forward Euler) was used for approximating the rest variables for the model. This means

TABLE I – THE PARAMETERS FOR PIHNA-LQ MODEL SIMULATION AND THEIR NONDIMENSIONALIZED VERSIONS

| Parameter  | Value  | Nondimensionalized                                      | Parameter | Value   | Nondimensionalized                       |
|------------|--|---|-----------|---|--|
| $\rho$     | $\frac{\ln 2}{\tau} \left( \frac{1}{\text{day}} \right)$                 | $\tau \rho = \ln 2$                                     | $\beta$   | $\frac{\rho}{10} \left( \frac{1}{\text{day}} \right)$               | $\frac{\ln 2}{10}$                       |
| $\gamma$   | $0.05 \left( \frac{1}{\text{day}} \right)$                               | $\tau \gamma = 0.0166$                                  | $D$       | $10^{-9} \left( \frac{\text{cm}^2}{\text{s}} \right)$               | $\frac{\tau}{L^2} D = 3 \cdot 10^{-5}$   |
| $a_n$      | $\frac{\ln 2}{50} \left( \frac{1}{\text{day}} \right)$                   | $\frac{\ln 2}{150}$                                     | $D_v$     | $10^{-9} \left( \frac{\text{cm}^2}{\text{s}} \right)$               | $\frac{\tau}{L^2} D_v = 3 \cdot 10^{-5}$ |
| $a_h$      | $\frac{\rho}{20} \left( \frac{1}{\text{day}} \right)$                    | $\frac{\ln 2}{20}$                                      | $D_a$     | $2.9 \cdot 10^{-7} \left( \frac{\text{cm}^2}{\text{s}} \right)$     | $\frac{\tau}{L^2} D_a = 8 \cdot 10^{-3}$ |
| $\mu$      | $\frac{\ln 2}{15} \left( \frac{1}{\text{day}} \right)$                   | $\tau \mu = \frac{\ln 2}{45}$                           | $K_m$     | $5.75 \cdot 10^{-7} \left( \frac{\text{mmol}}{\text{cm}^3} \right)$ | $\frac{K_m}{a_{\max}} = 10^{-3}$         |
| $\delta_c$ | $7.59 \cdot 10^{-16} \left( \frac{\text{mmol}}{\text{cell day}} \right)$ | $\frac{\tau k}{a_{\max}} \delta_c = 0.44 \cdot 10^{-4}$ | $\lambda$ | $\frac{\ln 2}{64} \left( \frac{1}{\text{min}} \right)$              | $\tau \lambda = 7.5 \ln 2$               |
| $\delta_h$ | $1.43 \cdot 10^{-12} \left( \frac{\text{mmol}}{\text{cell day}} \right)$ | $\frac{\tau k}{a_{\max}} \delta_h = 0.08$               | $\omega$  | $2.17 \cdot 10^{-6} \left( \frac{1}{\text{cell day}} \right)$       | $tk \omega = 72.33$                      |

that e.g. for the first equation that simulates the temporal change of  $c$ , the implementation uses Crank Nikolson for approximating  $c$  and its derivatives, grad and div, while it uses Forward Euler in order to approximate  $h, V, n$  and  $T$ . This holds similarly for the rest four equations of the non linear system.

## V. RESULTS

We have applied the PIHNA-LQ model for two cases. In the first case, the tumor is left to grow without treatment for 30 days, while in the second case radiotherapy is applied after 20 days of free growth for 10 more days. Table I depicts the parameters used in the model. The parameters used in the model were extracted from [12].

Before feeding the model with parameters, they were nondimensionalized according the formulas shown in the same table. The spatial nondimensionalization was built on a grid spanning an overall area of  $L \times L$  for  $L = 1\text{cm}$  and the temporal nondimensionalization was built on a time step of  $\tau = 8h$ . Thus, the new positions  $\hat{x}$  are found according to  $\hat{x} = \frac{x}{L}$  and the time is changed to  $\hat{t} = \frac{t}{\tau}$ . Lastly, the concentration  $c, h, n$  and  $v$  of normoxic, hypoxic, necrotic and endothelial cells, respectively, is nondimensionalized according to the capacity of cells  $k = 10^8 \frac{\text{cells}}{\text{cm}^3}$ , thus  $\hat{c} = \frac{c}{k}, \hat{h} = \frac{h}{k}, \hat{n} = \frac{n}{k}$  and  $\hat{v} = \frac{v}{k}$ . Similarly, the maximum value of angiogenesis is altered according to the formula  $\hat{a} = \frac{a}{a_{\max}}$ , where  $a_{\max} = 5.75 \cdot 10^{-4} \frac{\text{mmol}}{\text{cm}^3}$ .

For simulating radiotherapy, we set the LQ parameters as  $R = 60\text{Gy}$ ,  $A = 0.02\text{Gy}^{-1}$ ,  $B = A/10$  and  $OER = 3$ . For both simulation cases, the initial states for all five cell populations was set at:

$$\begin{aligned}
 \hat{c}(\mathbf{x}, 0) &= 0.93e^{-200(\mathbf{x}-\mathbf{x}_0)^2} \\
 \hat{h}(\mathbf{x}, 0) &= 0 \\
 \hat{n}(\mathbf{x}, 0) &= 0 \\
 \hat{v}(\mathbf{x}, 0) &= 0.01 \\
 \hat{a}(\mathbf{x}, 0) &= 0
 \end{aligned} \tag{6}$$

Row (a) of Fig. 2 presents the spatial concentration of normoxic, hypoxic and necrotic cells after 30 fictitious days of free glioma growth simulation. The computed graphs are depicted on a 40x40 grid (where  $L = 1\text{cm}$  and  $\mathbf{x}_0 = (20, 20)$ ). The row (b) depicts the respective graphs for the second case on the 30<sup>th</sup> day, assuming that radiotherapy treatment was applied for 10 days after 20 days of free growth (by applying the parameters of the previous section).

The results of our simulations computed that the peak value of the population of normoxic, hypoxic and necrotic cells is 0.7654, 0.2041 and 0.0139 in the case of free growth (PIHNA), while in the case of applying irradiation (PIHNA-LQ) these are 0.7614, 0.2906 and 0.8035 respectively. Moreover, the total viable cells ( $c + h$ ) on the 30th day decrease to 4.13k after therapy, compared to 5.23k for the case of free growth. Respectively, the total necrotic population ( $n$ ) increases during radiotherapy, as expected.

These results indicate that the numerical framework presented can model the effect of radiotherapy by incorporating the LQ model into the PIHNA model. PIHNA-LQ model needs to be validated in a quantitative fashion against actual clinical data before and after radiotherapy treatment is applied to specific patients. We are currently in the final stage of glioma dataset collection.

## VI. CONCLUSION

In this paper we presented an initial qualitative evaluation of a diffusion-reaction glioma growth model with normoxic, hypoxic and necrotic cells, incorporating vasculature, angiogenesis and radiotherapy treatment effect. We applied the Linear Quadratic model on the PIHNA model in two spatial dimensions.

The first results indicate that the radiotherapy can be simulated by this model. This is an important observation that needs further validation both from the experimental and the biological interpretation sides. Moreover, lysis of necrotic cells could be studied in future work by incorporating a subtraction term in the equation for necrotic cells.

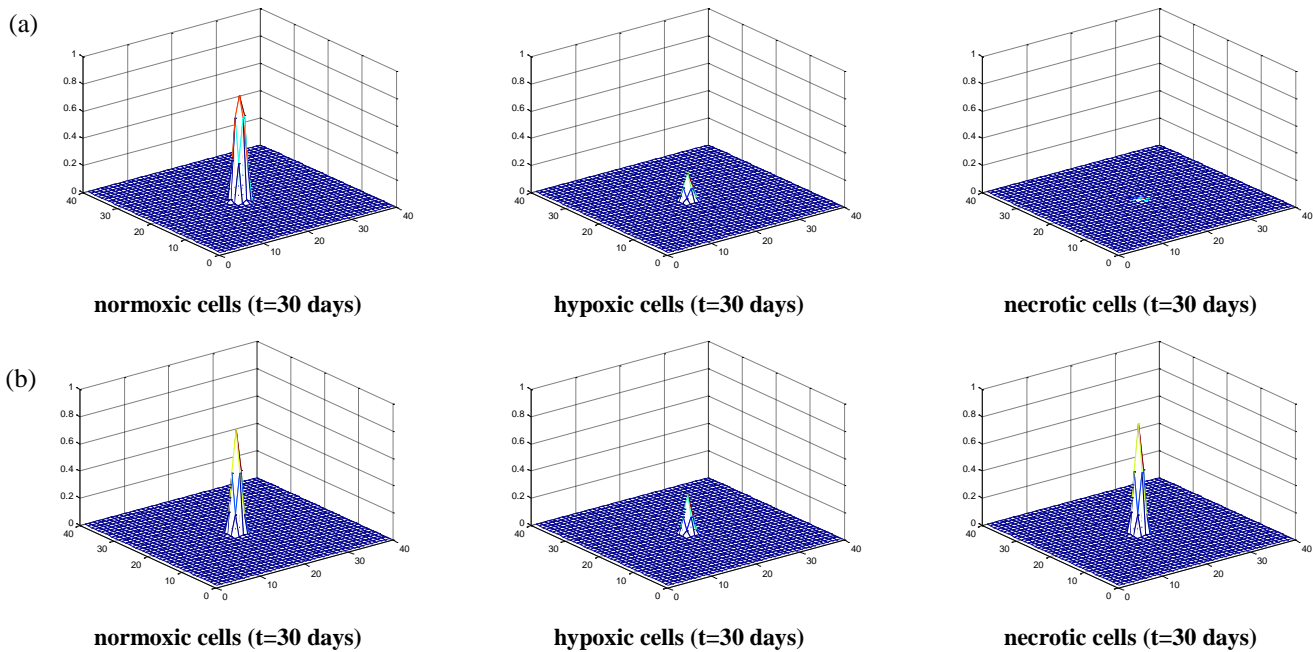


**Fig. 2.** The distribution of concentration for the three different populations of glioma cells (normoxic, hypoxic and necrotic cells) after applying the PIHNA model (a) and the PIHNA-LQ model (b). The graphs are extracted on the 30<sup>th</sup> day of simulation.

#### REFERENCES

- [1] WHO, "http://www.who.int/mediacentre/factsheets/fs297," World Health Organization. Retrieved 2012-09-15.
- [2] P. Boyle, and B. Levin, "World Cancer Report 2008," IARC, 2010.
- [3] Brain Tumors, "http://www.abta.org", American Brain Tumor Association. Retrieved 2012-09-15.
- [4] A. Roniotis, K. Marias, V. Sakkalis, and M. Zervakis, "Diffusive modeling of glioma evolution: a review," *JBiomSciEng, ScientRes*, vol. 3, no. 5, pp.501-508,2010.
- [5] A. Roniotis, G. Manikis, V. Sakkalis, M. Zervakis, I. Karatzanis, and K. Marias, "High grade glioma diffusive modeling using statistical tissue information and diffusion tensors extracted from atlases," *IEEE Trans Inform. Tech. in Biom*, vol. 16, no. 2, pp. 255-263, 2012.
- [6] A. Roniotis, V.Sakkalis, I.Karatzanis, M. E. Zervakis, and K. Marias, "In-depth analysis and evaluation of diffusive glioma models," *IEEE Trans Inform. Tech. in Biomedicine*, vol. 16, no. 3, pp. 299-307, 2012.
- [7] K. R. Swanson, E. C. Alvord, and J. D. Murray, "A Quantitative Model for Differential Motility of Gliomas in Grey and White Matter," *Cell Proliferation*, vol. 33, no. 5, pp. 317-330, 2000.
- [8] S. Jbabdi, E. Mandonnet, and H. Duffau, "Simulation of anisotropic growth of low-grade gliomas using diffusion tensor imaging," *MagnReson Med*, vol. 54, pp. 616-24, 2005.
- [9] O. Clatz, M. Sermesant, P. Bondiau, H. Delingette, S. K. Warfield, G. Malandain, and N. Ayache, "Realistic simulation of the 3-D growth of brain tumours in MR images coupling diffusion with biomechanical deformation", *IEEE Transactions on Medical Imaging*, vol. 24, pp. 1334-1346, 2005.
- [10] G. Stamatakos, V. Antipas, N. Uzunoglu, and R. Dale, "A four-dimensional computer simulation model of the in vivo response to radiotherapy of glioblastomamultiforme: studies on the effect of clonogenic cell density," *Br J Radiol*, vol. 79, pp. 389-400, 2006.
- [11] G. Stamatakos, V. Antipas, N. Ozunoglu, "A patient-specific in vivo tumor and normal tissue model for prediction of the response to P. Hinow, P. Gerlee, L. J. McCawley, V. Quaranta, M. Ciobanu, S. Wang, J. M. Graham, B. P. Ayati, J. Claridge, K. R. Swanson, M. Loveless, and A. R., Anderson, "A spatial model of tumor-host interaction: application of chemotherapy," *Math BiosciEng*, vol. 6, no. 3, pp. 521-46, 2009.
- [12] K. R. Swanson, R. C. Rockne, J. Claridge, M. A. Chaplain, E. C. Alvord Jr, and A. Anderson, "Quantifying the role of angiogenesis in malignant progression of gliomas: In Silico modeling integrates imaging and histology," *Cancer Res*, vol. 71, pp. 7366-7375, 2011
- [13] G. Steel, "Basic Clinical Radiobiology, 3rd Edition," Arnold, London, 2002.
- [14] E. Hall, "Radiobiology for the Radiologist," *J B Lippincott*, Philadelphia, 1994.
- [15] R. Rockne, J. K. Rockhill, M. Mrugala, A. M. Spence, I. Kalet, K. Hendrickson, A. Lai, T. Cloughesy, E. C. Alvord, and K. Swanson, "Predicting the efficacy of radiotherapy in individual glioblastoma patients in vivo: a mathematical modeling approach," *Phy Med Biol*, vol. 55, pp. 3271-3285, 2010.
- [16] A. Roniotis, K. Marias, V. Sakkalis, G. C. Manikis, and M. Zervakis, "Simulating radiotherapy effect in high grade glioma by using diffusive modeling and brain atlases," *J Biomed Biotech* (in press), 2012
- [17] L. Harrison, M. Chadha, R. J. Hill, K. Hu, and D. Shasha, "Impact of tumor hypoxia and anemia on radiation therapy outcomes," *Oncologist* vol. 7, no. 6, pp. 492-508, 2002.
- [18] J. Brown, and W. Wilson, "Exploiting tumour hypoxia in cancer treatment", *Nat Rev Cancer*, vol. 4, no. 6, pp. 437-47, 2004